Chapter 5
SURIYA System and Diagnostic Instruments

5.1 Introduction

The SURIYA beam transport line consists of two main parts; the Gun-to-Linac (GTL) section and the Linac-to-End of beam line (LTE) section. Figure 5.1 shows a schematic drawing of the top and side view of the beam transport line at SURIYA (April, 2006). At the GTL section, an RF-gun serves as an electron source where electrons are produced while the cathode is heated by an AC power supply. Electrons are accelerated or decelerated depending on the phase of the supplied RF-fields. The RF-gun was designed to produce and accelerate electrons such that high energy electrons concentrate at the head of the bunch followed by lower energy electrons leading to a monotonous energy-time correlation of the beam at the RF-gun exit. Details of the RF-gun design and construction are presented in Chapter 3 and 4. Downstream of the RF-gun there is an alpha-magnet (α-magnet) where bunch compression take place. In the α-magnet, the faster electrons travel along a longer closed path than the slower ones due to the alpha magnetic field. This method provides a simple and effective electron bunch compression. Inside the α-magnet vacuum chamber, two slits were installed as an energy filter. These energy slits are used to select electrons with a small energy spread which is very helpful in improvement of the electron beam transmission through the linac without a big loss. Moreover, the energy slits can be used to measure energies of electrons produced in the RF-gun.

To obtain higher electron beam energy and more radiation collimation, a SLAC-type linear accelerator was installed after the α-magnet to accelerate the electron beam to reach about 15-20 MeV depending on the supplied RF-power. The RF-gun and the linac are powered separately by a 5-MW klystrons with their associated modulators. There are several quadrupole and steering magnets placed along the beam transport line and serving as the beam focusing and steering elements in order to minimize the transverse dimension of the electron beam. There are three quadrupoles between the RF-gun and the α-magnet (Q1-Q3) and two quadrupoles (Q4-Q5) between the α-magnet and the linac. In the LTE

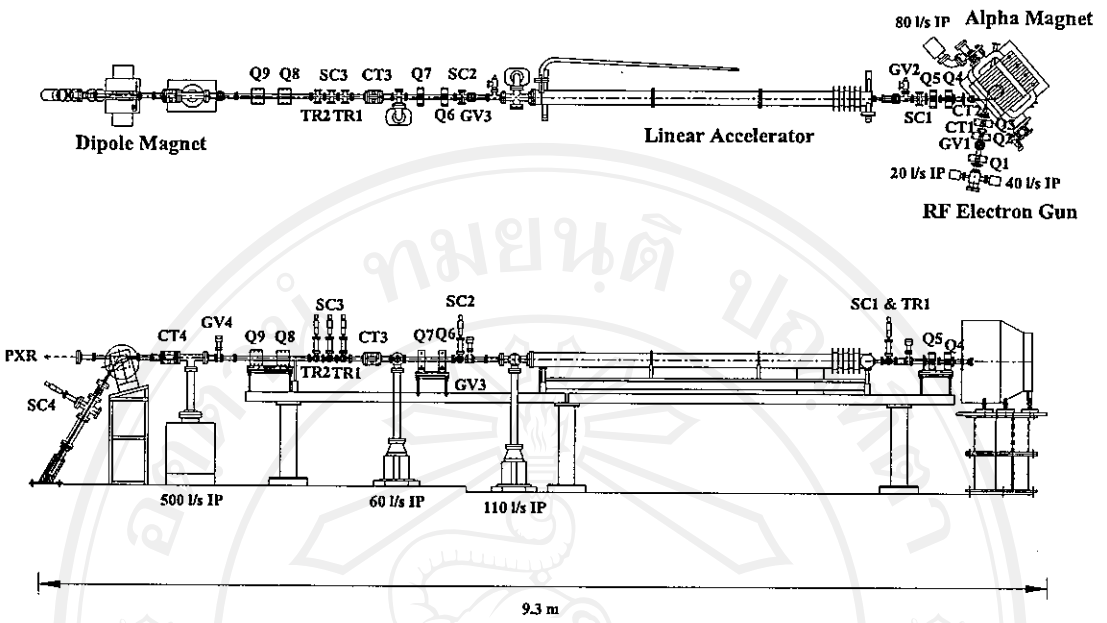

Figure 5.1. Top view and side view drawings of SURIYA beam transport system.

section, four quadrupole magnets (Q6-Q9) are installed in order to focus the electron beam at the experimental stations and guide the beam into the beam dump. There are eight pairs of steering magnets placing along the beamline; four in the GTL section and another four in the LTE section. Combination of a dipole magnet, a beam view screen and a Faraday cup are located at the end of the beam transport line serving as a beam dump element, a charge collector and an energy spectrometer.

Since ultra high vacuum environment is required for an electron accelerator several ion pumps are installed in the beamline to maintain a vacuum pressure of the order of 10^{-8} Torr. There are two gate-valves in the GTL section; one after the first quadrupole and another before the linac entrance. In the LTE section, one gate-valve is installed after the linac exit and another one before the entrance of the dipole vacuum chamber. These gate-valves allow for easy maintenance of the beamline components when necessary without breaking the vacuum in the RF-gun and in the linac. The cleanliness of the beamline components is extremely important for efficient system operation.

Several diagnostics are employed along the beam transport line to characterize the electron beam properties. To monitor the beam pulse current, two current monitors are located in the GTL section; one after the first quadrupoles

(CT1) and another after the α-magnet (CT2). Another two current monitors are installed in the LTE section (CT3 and CT4) for monitoring the beam current after the linac and before the beam goes into the dipole magnet vacuum chamber. There are three stations to generate the transition radiation; one before the linac (TR1) and another two after the linac (TR2 and TR3). Specifications and properties of the main beamline elements will be discussed in this chapter as well as the beam diagnostic instruments. Experimental station details for the production of transition radiation are presented in Chapter 7.

5.2 Magnetic bunch Compressor

An α-magnet serves as a magnetic bunch compressor [25] in the SURIYA system. The α-magnet is half a quadrupoles with two poles and a mirror plate replacing the other half. The α-magnet is an achromat element, while the lengths of the particle trajectory in the magnet exhibits a large dispersion depends on the particle energy and the magnetic field gradient. The α-magnet used at SURIYA has been designed and fabricated at FNRF based on its original design at Stanford SUNSHINE facility. Computer code POISSON [36] and MAGNET [52] were used to design the geometry and calculate the magnetic field of the α-magnet. Simulations show that a current of 265 A provides a gradient of 450 Gauss/cm [53]. This is sufficient for the electron bunch compression as described in Chapter 3.

Low carbon iron was used to build the magnet poles because of its high permeability. Nine plates of thick iron sheet were used to construct the whole magnet. The excitation coil had 70 turns of hollow copper wire. Measurement of the magnetic field gradient as a function of the excitation current was performed using a digital Hall Effect Teslameter and the results of the measured magnetic fields agree well with the calculations as shown in Fig.5.2. A water cooling system was built for the 3.7 kW power loss in the coils. With the water cooling, no significant temperature rise has been observed during the measurement [53]. There is a temperature sensor located at the α-magnet coils to measure the temperature during beam operation. There is a water flow rate interlock to prevent the magnet to be operated without water cooling. From our experience, the temperature of the magnet coils rises to a stable point of 37-38 ^{o}C when the magnet was excited with a current above 200 A for a few hours.

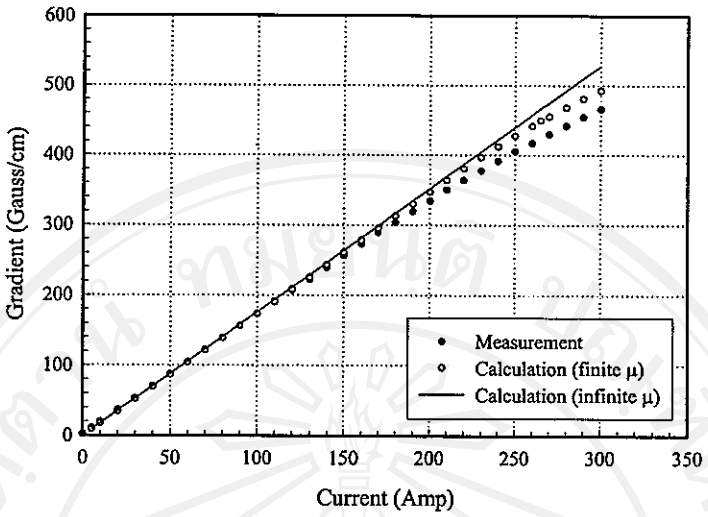

Figure 5.2. The α-magnet field gradients as a function of the excitation current.

The thermionic RF-gun produces a long low energy tail in the electron bunch (as discussed in Chapter 3). An energy slit inside the α-magnet vacuum chamber is used to reduce this energy spread by absorbing the low energy tail before it is further accelerated in a linac. It plays an important role in the improvement of the electron beam transmission through the linac since the low energy scrape absorbs useless low energy electrons. A schematic figure of particle trajectories inside the α-magnet and the energy slit (scrapers) is shown in Fig.5.3.

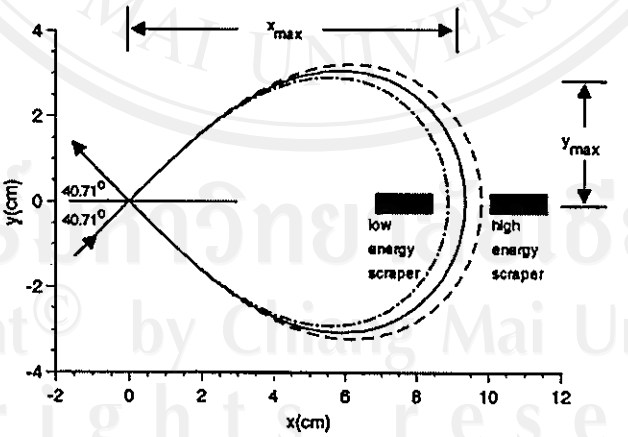

Figure 5.3. Particle trajectories inside the α-magnet with the energy slits [41].

In addition, the α-magnet energy slit can be used to measure the electron beam energy. Calibration of a mechanical counter on the scraper drive motors with the position of the scrapers in x-direction has been performed. The calibra-

tion provides the information of the maximum distance in x-direction (x_{max}) of the scraper edges from the vertex (the α-magnet entrance) and is related to the momentum of electron (cp) as

$$x_{max}(cm) = 75.05\sqrt{\frac{cp(MeV)}{mc^2 g(G/cm)}}, \tag{5.1}$$

where mc^2 is the electron rest mass and g is the α-magnet gradient. The high energy and the low energy scraper were calibrated on May 2004 and the calibration is

$$x_{max} = -1.043 + 5.328 \times 10^{-3} C \qquad for\ high\ energy\ scraper, \tag{5.2}$$

$$x_{max} = 12.114 - 5.132 \times 10^{-3} C \qquad for\ low\ energy\ scraper, \tag{5.3}$$

where C is the count of the motor counter. The electron energies before the linac acceleration as mentioned in this thesis were measured by the α-magnet energy slit and calculated from equations (5.1)-(5.3). The α-magnet slits are moved by the driver motor controlled by the software *Slit Control* [54]. This motor control and the software allows us to monitor directly the energy of the electron beam for different mechanical counters.

5.3 Linear Accelerator

Downstream of the α-magnet the electron beam is further accelerated in a linear accelerator (linac). The linac is a section of the SLAC linac structure with a length of 10 ft (3.048 m). This linac section was used as the post acceleration at the SUNSHINE system. It has a specific shunt impedance of 53 MΩ/m and the (unloaded) quality factor of 15000 [28]. The linac operating temperature is 45 ^{o}C for resonating at 2856 MHz. The linac is a constant gradient structure with a possible maximum kinetic energy gain (ΔE_{kin}) per 10 ft (3.048 m) in case of no electron beam loading as

$$\Delta E_{kin}[MeV] = 10.48\sqrt{P[MW]}, \tag{5.4}$$

where P is the RF-power delivered to the linac section. Since this linac is a travelling wave RF-structure it has an RF-power absorber at the end of the section to dump the remaining RF-power. With the available RF-power from the 5-MW klystron the maximum kinetic energy gain should be about 23.4 MeV.

5.4 Focusing and Beam Steering Elements

To maintain the electron beam in the beam transport system, focusing and beam steering elements are required. Quadrupole magnets are used as beam focusing elements. In addition, it can also be used for beam emittance measurements [55]. In this section the technical information of each quadrupole magnet in the SURIYA system is presented.

There are three different designs of quadrupole magnets used at the SURIYA beam transport line. Five quadrupoles (Q1-Q5) in the GTL section were designed as beam focusing components for a 3 MeV electron beam. These quadrupole magnets have a physical length, which is the length of the iron york, of 6 cm and the effective magnetic length is 7.75 cm [56]. In the LTE section, two quadrupole magnets are installed after the linac exit and used to focus the electron beam to the transition radiation stations (Q6-Q7). Both quadrupole magnets have the physical length of 6 cm with the effective length (from the trapezoidal approximation) of 7.8 cm [55]. The last set of the quadrupole magnets, with 11.4 cm physical length and 12.6 cm effective length [53], are used to guide the beam through the dipole vacuum chamber. All quadrupole magnets have a bore radius (the cross-section radius of the gap between the poles) of 2 cm. Measurements of the magnetic field gradient as a function of the applied current have been performed for all quadrupole magnets. From these results one can calculated the field strength of each quadrupole magnet. Details of each quadrupole magnets are compiled in Table 5.1.

Table 5.1. Some parameters for the quadrupole magnets using at SURIYA system.

Parameter	Q1-Q5	Q6-Q7	Q8	Q9
Phys. length(cm)	6.0	6.0	11.4	11.4
Eff. length(cm)	7.75	7.8	12.6	12.6
Bore radius(cm)	2.0	2.0	2.0	2.0
No. of coils (turns)	240	100	240	240
Max. current(A)	5	8	3	3
g(G/cm) vs. I(A)	$140.53I$+6.74	$49.31I$+17.84	$147.37I$+3.63	$148.21I$+4.52

Several steering beam elements are installed in the SURIYA beamline. Four square-frame steering magnets, used in the GTL section, were constructed

from four-iron bars with 17 turns of copper-wire wound on each bar [55]. Figure 5.4 shows a schematic diagram of the square-frame steering magnet used in the GTL section. Each pair of steering magnets was designed for correcting the 3 MeV electron beam both in the horizontal and vertical direction. Two coils on opposite sides are energized to produce a magnetic field in the same direction. The fields from both coils collide at the bar between the coils and are forced to flow through the gap as shown in Fig.5.4. The vertical magnetic field is used for deflecting the electron beam in horizontal direction and vise versa the horizontal magnetic field is used for deflecting the electron beam in vertical direction. The net steering magnetic field of each pair is determined by the superposition of the field generated from each coils. The deflecting angle from the steering magnet is limited by the excitation current supplied to the magnet. At SURIYA, the GTL steering magnet power supplies can provide a maximum current at about 2 A leading to a maximum deflecting angle of 3.5^{o} [55]. The steering magnets used in the LTE section are small air-coil dipoles which can deflect a higher energy electron beam than the four-frame steering magnet. Contrary to the four square-frame steering magnet, the horizontal magnet produces vertical magnetic field and the vertical magnet produces horizontal magnetic field. Figure 5.5 shows the horizontal steering magnet (left) and the vertical steering magnet (right) and their fields.

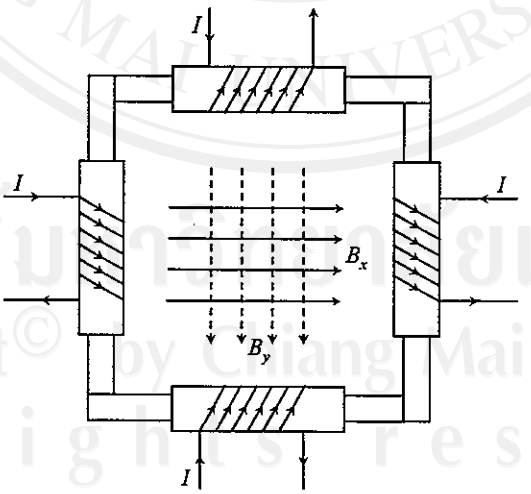

Figure 5.4. Schematic diagram of square-frame steering magnet with its fields. The horizontal magnetic fields B_x (solid lines) deflect electron in vertical direction and the vertical magnetic fields B_y (dash lines) deflect electron on horizontal direction.

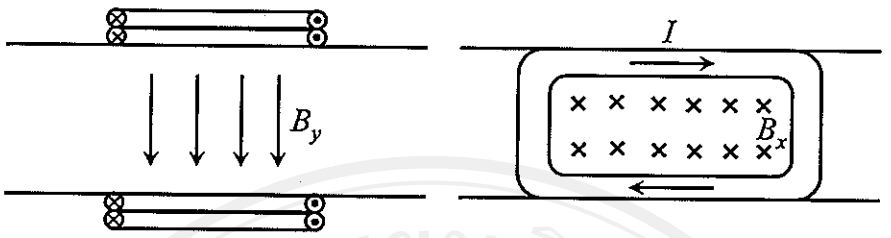

Figure 5.5. Schematic diagram of a small air coil dipole steering magnet with its fields.

5.5 RF Power System

As discussed in Chapter 2 electromagnetic waves must be supplied to the resonant cavity in order to excite the cavity and accelerate electrons. In case of a pulsed beam like our system, a pulsed RF-source is required. A klystron is a suitable source for our case due to its high gain amplifier, high efficiency and long life time with a reliable frequency stability. The klystron is an RF-amplifier, which needs an input signal and input electrical power. The input RF-signal is generated by a low power RF-oscillator and then amplified by a pre-amplifier. The input electrical power is generated by a RF-modulator system. At the SURIYA facility, the RF-gun and linac are powered by two separate RF sources consisting of a common low power RF-oscillator and two 5-MW klystrons with their associated modulators. A schematic layout of the SURIYA RF-system is illustrated in Fig.5.6.

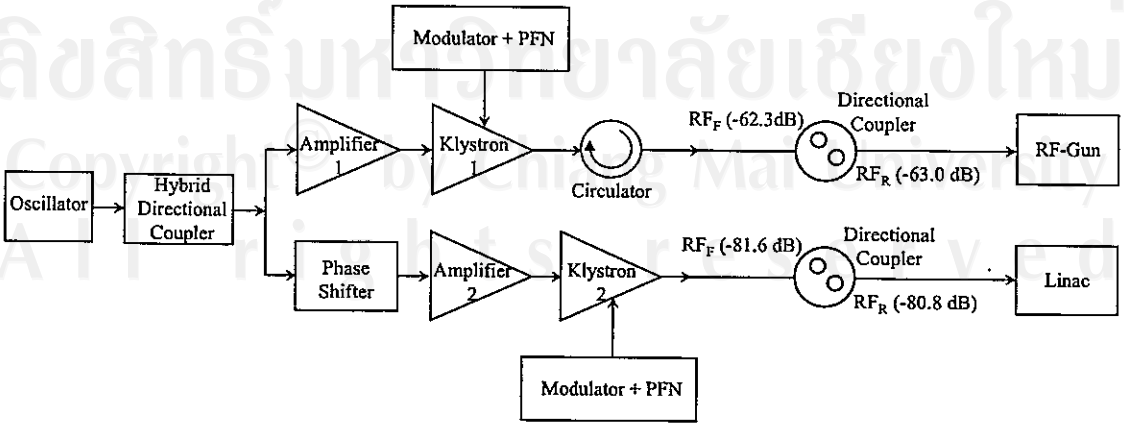

Figure 5.6. Schematic layout of SURIYA RF-system.

5.5.1 Low-Level RF-System

A low-level RF signal is generated by a commercial tube 3CPX100A5 in a resonant tank oscillator and the resonant frequency is tuned to 2856 MHz by a standard cavity. The end plate of the standard cavity can be adjusted to be moved in and out by a motor to change the resonant frequency. The oscillator unit produces an RF-signal of 40 W average power. The RF-signal is then split into two signals by a 3 dB 90° hybrid directional coupler. One feeds the gun RF-amplifier and the other the linac amplifier through an adjustable phase shifter. The phase shifter can be adjusted manually from the control room with a scale readout, which can be adjusted in the range of 180° per 1 GHz. Figure 5.7 shows the low-level RF system consisting of the RF-oscillator unit, the 3 dB 90° hybrid directional coupler and the adjustable phase shifter.

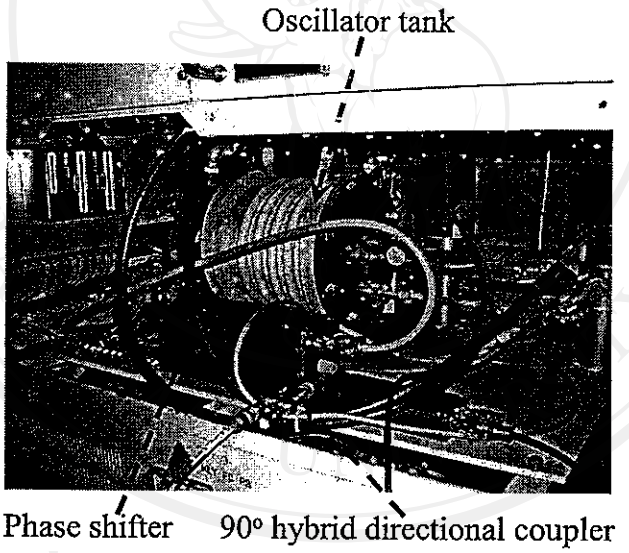

Figure 5.7. Low-level RF system consisting of the RF-oscillator, the 90° hybrid directional coupler and the adjustable phase shifter.

Both RF-amplifiers for the RF-gun and the linac produce an RF-output pulse when the RF-signal is trigged with a signal originally produced from a separate master trigger box in their individual control units. The output signal is about 100 W at maximum RF-pulse duration of 8 μs (FWHM). The width of the RF-pulses can be adjusted by varying the number of capacitors in the pulse forming network (PFN) units. The PFN has a parallel network of 8 capacitors and 8 inductors. The PFN is charged and discharged using a deuterium thyratron switch model CX-1524A.

5.5.2 RF-Amplify in Klystron

At SURIYA, both klystrons for the RF-gun and the linac are commercial Mitshubishi models. The klystron with related modulator system driving the RF-gun was available from the Sirirat Hospital medical linac by donation while the one driving the linac was donated by the Chiang Mai Hospital. The klystron is an RF-amplifier consisting of a klystron tube, focusing coil and high voltage pulse transformer in insulating oil. The klystron is a straight vacuum tube consisting of a thermionic electron gun with a DC-accelerating cavity, an input cavity (or called bunching cavity), a drift space and an output cavity. An electron beam is generated from the thermionic cathode inside the klystron tube. The RF-pulse output from the RF-amplifier is sent to the bunching cavity of the klystrons. A high-current, high-voltage pulse from the modulator drives the pulse transformer in the klystron tube. In the bunching cavity the electron beam is velocity modulated by the RF-input signal. The velocity modulation is converted into a current modulation at 2856 MHz in the drift space after the bunching cavity. During klystron operation the electron beam diverges due Coulomb force, which will be prevented by focusing coils around the klystron tube. An output cavity is placed at a position where the current modulation in the electron beam is maximal. High-intensity RF-power is extracted from the output cavity and enters a waveguide through a ceramic RF-window. The klystron acts as an amplifier producing about 5-MW peak power at 2856 MHz in a 8 μs (FWHM) pulse (5-6 μs flatted-top) with an average driving power of 250-300 W. The repetition rate of the RF-pulse was typically 10 Hz. Relation of the average power (P_{ave}) and the peak power (P_{peak}) from the klystron can be calculated from

$$P_{ave} = (\tau)(pps)(P_{peak}), \tag{5.5}$$

where τ is the RF-pulse width and *pps* is the pulse repetition rate. The schematic picture of the klystron tube is shown in Fig.5.8. The actual klystron tube is mostly invisible located inside a magnet and lead housing for x-ray shielding.

Klystron operation is critically controlled by three requirements; stable high-voltage power supply, sufficient water cooling and high-vacuum condition. Water cooling is required at all time during klystron operation since there is a large heat load at the absorber of the klystron due to the residual energy of electron beam. The water cooling system is divided into two lines for the klystron

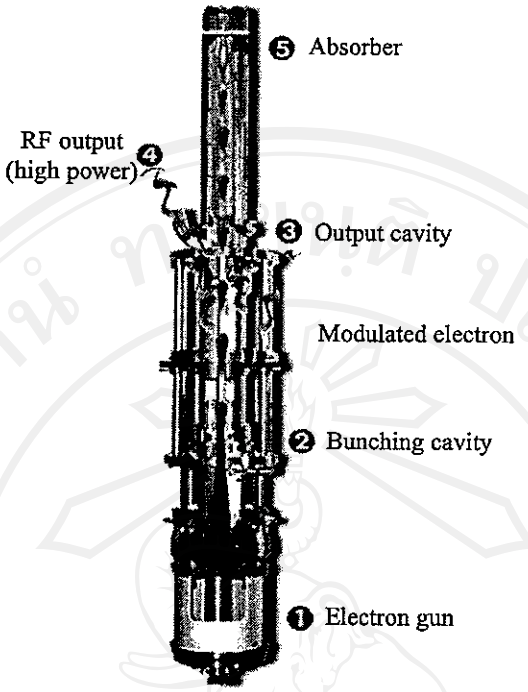

Figure 5.8. Schematic picture illustrates the main components of the klystron tube [57].

body and the klystron focusing coil. The high-voltage supply to the klystron is interlocked with the cooling water temperature and flow rate to prevent excessive heat in the klystron while in operation. In addition, since the klystron works as an amplifier driven by an electron beam a vacuum environment is required. To maintain a high vacuum lower than 10^{-7} Torr, a 20 l/s ion pump unit is attached to both klystron tubes. A ceramic RF-window is located at the exit of the output cavity of the klystron to separate the klystron tube from the rest of the waveguide system.

5.5.3 RF-Power Transmission to Accelerator

The high-level RF-power is transmitted to the RF-gun and the linac through a WR-284 rectangular waveguide system pressurized with sulfur hexafluoride (SF_6) to prevent electrical discharges. SF_6 is an inert and heavy gas which can inhibit the RF-breakdown by resisting ionization. The pressure of SF_6 must be monitored and kept at 1.5 bar during klystron operation. A high-power ceramic RF-windows is placed between the rectangular waveguide system and the accel-

erator (the RF-gun and the linac) to isolate the SF_6 filled waveguide section from the evacuated section. The RF-window is a pillbox type, using a half-wavelength of aluminum disk coated with titanium on both sides to suppress multipactor heating. Leaking of the RF-window can be monitored by the pressure in the ion pump units connected to the RF-gun and the linac.

Since the RF-gun is a standing-wave structure it reflects the RF-power at the beginning and the end of the RF-pulse. A 4-port circulator is placed after the klystron output cavity to protect the klystron from the reflected RF-power. It also protect the klystron from reflections from breakdown phenomena. The first port of the circulator is connected to the klystron, the second port is connected to the waveguide to RF-gun and another two ports are terminated by a matched load. The reflected RF-power is absorbed into the dummy load to keep the klystron tube safe at all time of operation. There is no need of the circulator for the linac because the linac is a travelling-wave structure which the RF-wave being dumped in the absorber at the linac exit.

5.5.4 How to Measure RF-Power

The RF-power is measured using directional couplers with crystal RF-detectors on the waveguide section to the RF-gun and the linac. An accurate RF-power measurement requires knowledge of the coupling strength between the waveguide, the accelerating cavity and the diagnostic ports. Forward and reflected port attenuation to the directional couplers for the RF-gun and the linac were measured and calibrated by using a network analyzer and the measured values are shown in Fig.5.6. Both the RF-power flowing forward to the accelerator and the reflected power were measured at the directional coupler and sent to the control room through low-loss RG-228 cables. These RF-signals are converted to be a DC-voltage signals by calibrated crystal detectors and monitored by a digital oscilloscope.

The crystal detector is a diode that rectifies the RF-signal and produces a DC-voltage output. The crystal detectors used at SURIYA are Hewlett Packard model CD 423A and CD 423B, which have an RF input limit of 200 mW. Normally, the forward and reflected RF-power from the directional coupler is much higher than this detector limit. Hence, calibrated attenuators must be added to the crystal detector to prevent excessive RF-power damaging the crystal detector. All

crystal detectors at SURIYA have been calibrated using a network analyzer as an RF-generator and a voltmeter as a DC-voltage readout. From calibration data, it was found that the crystal detector voltage is linearly proportional to the input RF-power in the range of 100-380 mV. Hence, any measured input power in this range can be calibrated linearly. The DC-voltage output from the crystal detector is observed on the oscilloscope and the actual RF-power value at the directional coupler can be calculated with the calibration of the crystal detector taking into account the amount of attenuation from the directional coupler, transmission cable and the attenuators.

5.6 Beam Diagnostic Instruments

Several diagnostic instruments have been installed in the SURIYA system to characterize the electron beam qualities. Current transformers are used to measure the beam current and pulse length. Several phosphor screens are installed along the beam transport system to monitor the transverse beam size. An energy slit inside the α-magnet vacuum chamber is used to measure the energy and energy spectrum of the electron beam produced by the RF-gun and at the end of the beamline a combination of a dipole magnet, a phosphor view screen and a Faraday cup is used to measure the beam energy after linac acceleration and the total electron charge.

5.6.1 Current Monitor

The electron pulse current and its length is measured with a ferrite-core toroid around the beam path. This toroid functions as the inductive core of a transformer and is therefore called a *beam current transformer*. The most advantage of current transformer is due to its a nondestructive property since the electron beam is just passing through the current transformer without stopping or losing intensity or energy. The fundamental physics behind the current transformer will be discussed as follow. The electron beam current I_b acts as the current in the primary coil and the secondary coil of N_s turns around the ferrite core is used for measuring the output current signal I_s. The toroid is mounted over a ceramic insulator inserted in a stainless steel vacuum tube to avoid image current which would cancel the beam current signal. The magnetic field (B_{loop}) produced

by the beam current induces a current in the secondary coil which is proportional to B_{loop}. Then, we get

$$\frac{\mu_0 I_s N_s}{2\pi\rho} = \frac{\mu_0 I_b N_b}{2\pi\rho}, \tag{5.6}$$

where ρ is the toroid radius. Equation (5.6) can be rewritten in a simple form as

$$I_b = N_s I_s, \tag{5.7}$$

because N_b=1. The current I_s produces across a resistor R, the voltage V_s, and the beam current (I_b) becomes with (5.7)

$$I_b = \frac{N_s}{R} V_s, \tag{5.8}$$

where V_s is the signal voltage measured by oscilloscope. In SURIYA system most of the current transformers have a secondary coils of 8 turns and use a resistive load of 50 Ω, hence the practical formula for convenient measurement is

$$I_b = \frac{8}{50} V_s = 0.16 V_s. \tag{5.9}$$

The schematic model and the actual picture of the current transformer used at SURIYA are shown in Fig.5.9.

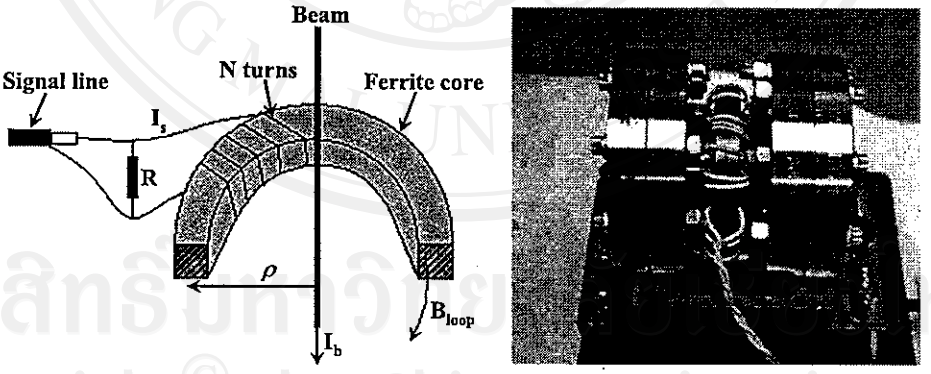

Figure 5.9. Schematic model of current transformer (left) [55] and actual current transformer using at SURIYA (right) with a metallic shield taken off.

5.6.2 Beam Viewer Set Up

Phosphor screen with an air pressure actuator is a simple instrument for monitoring the beam profile and measure the transverse dimension of the electron

beam. The screen is inserted into the vacuum tube at an angle of 45^o with respect to the beam axis and is illuminated by fluorescence when electron beams are passing through. The beam image is viewed by a CCD camera connected to a computer with an image capture program. The view screen measurement setup is shown in Fig.5.10. The phosphor screens used in the beam profile measurement in this thesis are homemade. It is made of phosphorescent material ($Gd_2O_2 : Tb$) deposited on a thin aluminum plate with a grain size of 8-10μm [58].

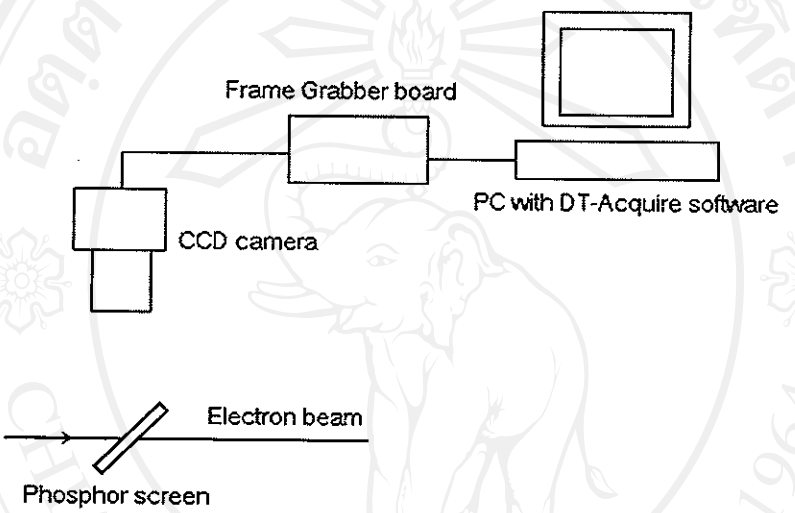

Figure 5.10. Schematic layout of beam profile measurement set up [55].

At the early stage of SURIYA operation, the beam image was detected by a CCD camera and displayed on a PC monitor. The window software (DT-Acquire), compatible with the frame grabber card (DT3315 Data-Translation), has been installed to capture and save the image to hard disk. The image was analyzed for the relative transverse bunch distribution and its transverse size with MATLAB code BAP [55]. To obtain the actual beam size, the calibration of the actual size and the image size is required. Later, the PC for control and experiment was upgraded to be more efficient and more reliable, a most modern computer model and the Window XP operating system were used. Since the frame grabber board (DT3315 Data-Translation) was not compatible with the window XP operating system it was replaced by the *TV Tuner* card which can be used to capture a still image or to record in the video mode. However, the phosphor screen measurement setup for viewing the electron beam setup is still the same.

5.6.3 Dipole Magnet as Beam Dump and Energy Spectrometer

At the end of the beam transport system, there is a dipole magnet serving as an electron beam dump. The dipole magnet has been designed to deflect an electron beam 60° into a Faraday cup. A C-shape dipole magnet has been modified from a 270° magnet of the hospital therapy linac. The modification was made only to its poles [53]. The square cross-section (12.5 cm × 12.5 cm) pole profile with a gap between the poles of 8 cm was designed and simulated using the RADIA code [59]. 3D-model of the dipole magnet in Fig.5.11 (left) shows that electrons propagate in yz-plane in the dipole magnetic field. To use the dipole magnet as an energy spectrometer, a three dimensional magnetic field measurement was performed and the results are shown in Fig.5.11 (right).

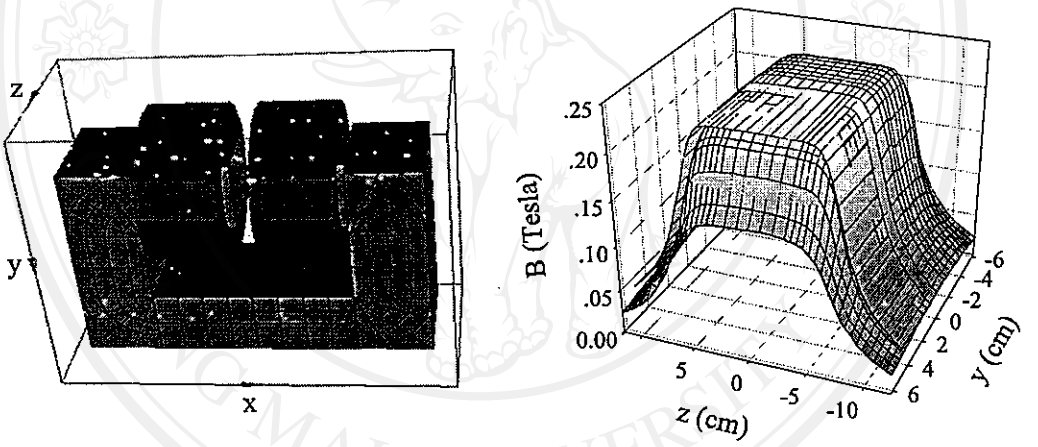

Figure 5.11. 3D-view of dipole magnet (left) and 3D-measured magnetic field map for the dipole magnet (right).

A vacuum chamber was installed between the magnet poles with one entrance and two exit ports; one in the propagation direction of the incoming beam and another making an angle of 60° with respect to the beam direction. The view screen set up was placed after the 60° exit port of the vacuum chamber for monitoring the electron beam image. The energy measurement can be performed at this view screen and the energy resolution is limited by the screen size. A Faraday cup was installed at the very end of the beamline to detect the total electron charge. The combination of the dipole magnet, the view screen set up and the Faraday cup provides an instrument for the electron energy measurement and the electron charge monitor. The schematic drawing of the vacuum chamber, the view screen

set up and the Faraday cup is shown in Fig.5.12.

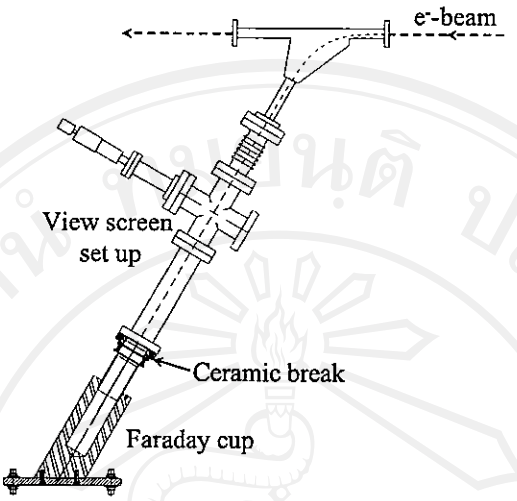

Figure 5.12. Design drawing of the vacuum chamber of the dipole magnet, the view screen set up and the Faraday cup.

The electron total energy (E) can be calculated from the deflection angle of electron in the dipole field as [28]

$$E\ [GevV] = \frac{0.2998 \int B_y(z)dz\ [Tesla \cdot m]}{\beta\alpha\ [radian]}, \tag{5.10}$$

where $\int B_y(z)dz$ is the magnetic field along the electron path and α is the deflecting angle, which is 60^o or $\pi/3$ radian in our case. For a relativistic electron beam, like in our case, $\beta = v/c \approx 1$. Practically, the only parameter that can be observed while the dipole magnet and the SURIYA system are in operation is the excitation current to the magnet. A measurement of dipole magnetic fields as a function of the excitation current was performed and the result is shown in Fig.5.13 (left) and the relation of the calculated energy as a function of excitation current is shown in Fig.5.13 (right). These calculated energies of the electron beam were simulated by using the computer code *Trajectory Simulator* [60]. The results in Fig.5.13 (right) show that the dipole magnet can function as the energy spectrometer for the electron energies of 2 to 41 MeV with a magnet current of 0.5 - 16.5 A. Since the maximum energy of the electron beam that can be reached after the linac acceleration (described in section 5.3) is about 26 MeV (2.5 MeV from RF-gun and 23.5 MeV from linac acceleration) an excitation current of about 11 A is required to deflect this high energy electrons. With this high current water

cooling for the magnet coils is needed. The coils of the dipole magnet are hollow copper tubes that allow the cooling water to flow through during magnet operation. For accurate energy measurements the dipole magnet has been well aligned with respect to the beam line and the vacuum chamber by using an alignment telescope.

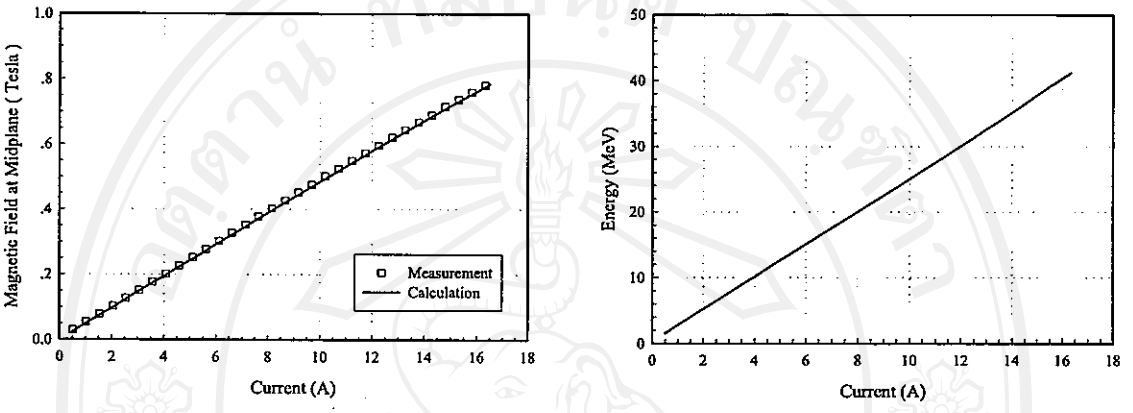

Figure 5.13. Measured Maximum magnetic field in the dipole magnet as a function of excitation current(left) and calculated energy of the electrons as a function of the excitation current of the dipole magnet (right).

The electron charge is measured with a Faraday cup to collect the beam charge and an oscilloscope to integrate over the current pulse signal. The Faraday cup at SURIYA has a long core of 19 cm in length with the copper wall thickness of about 2.5 cm to absorb all electrons. The whole Faraday cup is isolated from the rest of the system to allow the calculation of the charge signal. The diameter of opening entrance of the core is 5.7 cm and it limits the resolution of the energy measurement. The Faraday cup is connected to a coaxial feedthrough with a BNC connector to connect to the oscilloscope. A 50 Ω load is connected to the Faraday cup when the measurements take place. There is a ceramic gap between the copper core and the stainless steel vacuum tube to prevent electrical contact which would prohibit charge measurement.